

# Silica-coated quantum dots and magnetic nanoparticles for bioimaging applications (Mini-Review)<sup>a)</sup>

Subramanian Tamil Selvan<sup>b)</sup>

*Institute of Materials Research and Engineering, 3 Research Link, Singapore 117602, Singapore*

(Received 30 August 2010; accepted 23 October 2010; published 14 December 2010)

Fluorescent quantum dots (e.g., CdSe–ZnS) and magnetic nanoparticles (e.g., Fe<sub>2</sub>O<sub>3</sub> or Fe<sub>3</sub>O<sub>4</sub>) are two important candidate systems that have been emerging as potential probes for bioimaging applications. This review focuses on the development of silica-coated inorganic probes (optical and magnetic) that are originated mainly from the author's laboratory for bioimaging applications. The recent developments in the synthesis of rare earth nanoparticles for multimodality imaging are also delineated. © 2010 American Vacuum Society. [DOI: 10.1116/1.3516492]

## I. INTRODUCTION

Inorganic nanoparticles (NPs) for biomedical applications have advanced rapidly in recent years due to their excellent optical and magnetic properties. Over the past several years, quantum dots<sup>1–9</sup> (QDs) and magnetic nanoparticles<sup>10–13</sup> (MPs) have been emerging as inorganic based optical and magnetic bioprobes, respectively. The magnetofluorescent NPs are potential candidate systems for *in vivo* imaging, which can be detected by imaging techniques such as magnetic resonance imaging (MRI), fluorescence imaging, tomography, confocal microscopy, and flow cytometry.

Highly fluorescent semiconductor QDs (e.g., CdSe–ZnS) have emerged as a potential fluorescent label owing to their remarkable optical properties. Compared to fluorescent dyes, QDs do not have the setback of photobleaching, and their emission colors can be tuned from visible to near-infrared (NIR) region by varying the size or composition of QDs. A significant research effort has been devoted to prepare core-shell type QDs with a cross-linked shell that would protect the QDs much better than thiol-based coating. The most widely used approach is silica coating<sup>14–19</sup> among other methods such as ligand or polymer bridging.<sup>20</sup> Although a variety of functional NPs or QDs have been synthesized by silica or polymer coating, each coating method has inherent advantages and limitations. It would be ideal to have a thin, cross-linked coating that could protect the core, improve colloidal stability, and introduce chemical functionality for bioconjugation.<sup>21</sup> Efforts are still underway in various groups in order to make a library of robust functional NPs.

Conversely, MPs are used as contrast agents in MRI applications. Generally, there are two types of contrast agents (positive and negative), which are dictated by the shortening of longitudinal or transverse relaxation times of water protons, resulting in either brightening or darkening of magnetic resonance images for T<sub>1</sub> and T<sub>2</sub> weighted imaging, respectively. The typical examples of T<sub>2</sub> contrast agents are

γ-Fe<sub>2</sub>O<sub>3</sub> (maghemite), Fe<sub>3</sub>O<sub>4</sub> (magnetite), Co, and MFe<sub>2</sub>O<sub>4</sub> (M=Ni, Co, Fe, and Mn), and those of T<sub>1</sub> contrast agents are gadolinium (Gd)-chelates [Gd-diethylene triamine pentaacetic acid (DTPA)] and Gd<sub>2</sub>O<sub>3</sub>.

The bifunctional probes offer great advantages for optical and magnetic based imaging applications. The magnetofluorescent NPs, or in short magnetic QDs, are useful for fluorescence based labeling applications, magnetic based cell harvesting, tracking, and drug targeting, and MRI applications. The synthesis of these bimodal magnetic-fluorescent probes has received great interest in recent years. Over the years, we have been interested in the assemblies of QDs or MPs within a shell consisting of either silica or polymers. Herein, we briefly review our recent work on the progress of silica-coated QDs and MPs for biolabeling and MRI applications. We also highlight the recent demonstration of rare earth (RE) based down- and up-conversion NPs (UCNPs) for multimodality imaging.

## II. FLUORESCENT QUANTUM DOTS FOR CELL LABELING

There are three important stages before the QDs can be utilized for biological applications: (a) synthesis, (b) coating, and (c) surface functionalization or bioconjugation, as depicted in Scheme 1. This scheme is common for metal NPs (e.g., Au and Ag) and semiconducting QDs (CdSe/ZnS) for applications in biosensing and bioimaging, respectively.

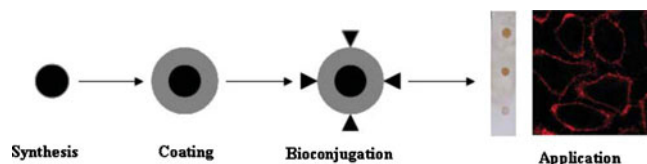
### A. Synthesis and coating strategies

In general, the high-temperature organometallic route produces high-quality QDs. The as-synthesized QDs are not water-soluble as they are capped with organic surfactants such as trioctylphosphine oxide (TOPO) and hexadecyl amine. Nevertheless, for practical biological applications, the hydrophobic QD surface needs to be rendered hydrophilic and amenable to surface modification and functionalization. Silica surface meets these requirements. However, because of the ultrasmall sizes of QDs, it is extremely difficult to achieve silica coating of single QDs via the Stöber process.

Water-soluble functional NPs are indispensable for various biomedical applications. However, the synthesis of ro-

<sup>a)</sup>This article is part of an In Focus section on Biointerphase Science in Singapore, sponsored by Bruker Optik Southeast Asia, IMRE, the Provost's Office and School of Materials Science and Engineering of Nanyang Technological University, and Analytical Technologies Pte., Ltd.

<sup>b)</sup>Electronic mail: subramaniant@imre.a-star.edu.sg



SCHEME 1. (Color online) General steps involved toward the application of QDs.

bust functional NPs is very challenging, since most of the good synthetic methods available for noble metal, QD, and magnetic oxides produce hydrophobic NPs because of hydrophobic surfactant coating. Thus, water solubilization and functionalization are the key issues prior to their application and here lies the significance of coating.<sup>20,22</sup> The coating helps convert hydrophobic NPs into hydrophilic water-soluble particles and introduces chemical functionality to the particle surface so that different chemicals and biomolecules can be covalently attached. There are two common coating strategies to convert hydrophobic NPs into hydrophilic and functional NPs. The first approach involves the ligand exchange of the original surfactant by hydrophilic ligands such as thiols or other functional groups.<sup>23</sup> Thiol-based ligand exchange is most common for noble metal NPs compared to other systems. This is because thiol makes a strong chemisorption on noble metal surface. In addition, various approaches of thiol-based methods were developed to make a stable coating, which involves the use of ligands with either multiple thiols, thiolated dendrimers, dendrons, or cross-linking of surface ligands.<sup>1,10</sup>

The second approach involves the interdigitated bilayer formation between amphiphilic molecules/polymers and the passivating surfactant layer surrounding NPs.<sup>24</sup> These approaches have been successfully applied to noble metal NPs, in comparison with iron oxide MPs and QDs. Several methods exist in the literature on the design of water-soluble QDs.<sup>24–27</sup> One method involves an organic coating using either polymers,<sup>25</sup> micelles,<sup>26</sup> or thiols<sup>27</sup> as the linker molecules. Another method is based on the well-known silica chemistry developed for coating metal NPs.<sup>28</sup>

## B. Direct coating of hydrophobic semiconductor QDs

Silica coating is one of the facile approaches to render the QDs with characteristic properties such as water solubility, moderate buffer stability (more stable under alkaline conditions), and photostability.<sup>14</sup> There are two ways to prepare silica-coated QDs: (a) thin silica coating (<10 nm) by silanization and (b) thick silica coating (>10 nm) by the Stöber method. Earlier, we synthesized 20–30 nm silica-coated CdSe/ZnS QDs via a reverse microemulsion.<sup>5</sup>

The as-synthesized hydrophobic ZnS-capped CdSe QDs can be coated with silica in a direct one-pot reverse microemulsion method, employing Igepal as the nonionic surfactant.<sup>5</sup> Initially, reverse micelles were synthesized using Igepal and cyclohexane as nonionic surfactant and solvent, respectively. We have developed a simple strategy for making plain CdSe QDs (without ZnS capping) water-soluble by

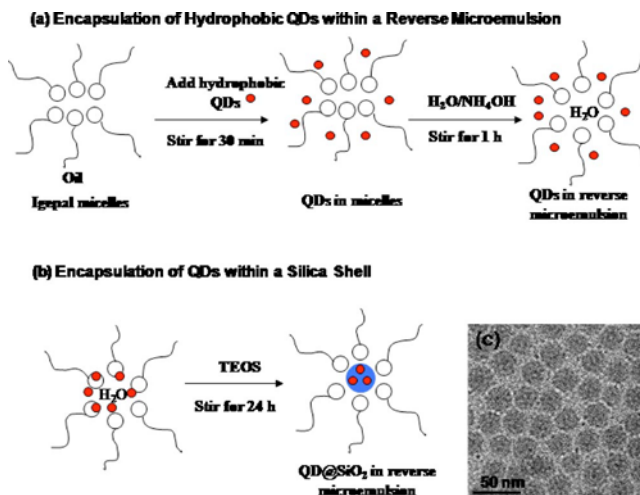


FIG. 1. (Color online) Synthesis of silica-coated quantum dots. (a) Encapsulation of hydrophobic TOPO-capped CdSe–ZnS QDs within a reverse microemulsion and (b) within a silica shell. (c) TEM image of multiple QDs encapsulated within silica shells.

silica coating. The surfactant interaction prior to silica coating allows the hydrophobic QDs to be encapsulated within the aqueous domains of the reverse microemulsion (Fig. 1). This involves the hydrophilic groups of TOPO and Igepal CO-520, which are surfactants present on the QD surface and in the reverse microemulsion, respectively.

This direct silica coating approach has enabled a wide variety of hydrophobic NPs or QDs (e.g., CdSe and PbSe), magnetic NPs (e.g.,  $\text{Fe}_2\text{O}_3$ ), and bifunctional NPs or heterodimers (e.g., CdSe–ZnS/ $\text{Fe}_2\text{O}_3$ ) to be encapsulated within spherical silica particles.<sup>5,6,19,29</sup> At first, NPs have to be transferred to the hydrophilic interior of micelles where silica growth takes place. The particle bearing a hydrophobic surface has to be exchanged with a hydrophilic ligand. The mechanism of transfer is clearly elucidated in a recent article.<sup>30</sup> The TOPO-capped QDs were introduced to the reverse micelles, where Igepal could be exchanged partially or completely with TOPO. The addition of a base, ammonia, forms a reverse microemulsion [Fig. 1(a)]. The QDs are still present in the oil phase. After the addition of a silane [tetraethoxy silane (TEOS)], hydrolysis and condensation occur, resulting in the encapsulation of QDs within a silica shell, as depicted in Fig. 1(b). This simple silica coating strategy enabled us to prepare water-soluble, plain CdSe QDs (without ZnS capping). The typical transmission electron microscopy (TEM) image of silica-coated QDs is shown in Fig. 1(c).

## C. Live cell imaging

Recently, we developed silica-coated QDs for live cell imaging.<sup>6</sup> Silanization in reverse microemulsion produced a thin silica coating on bare CdSe QDs with surface  $\text{NH}_2$  groups [Fig. 2(a)]. The addition of aminopropyl triethoxysilane (APS) introduced amine groups that were attached to the surface of QDs. With the sequential addition of tetramethylammonium hydroxide in 2-propanol/methanol and water, a reverse microemulsion was formed. The methoxy

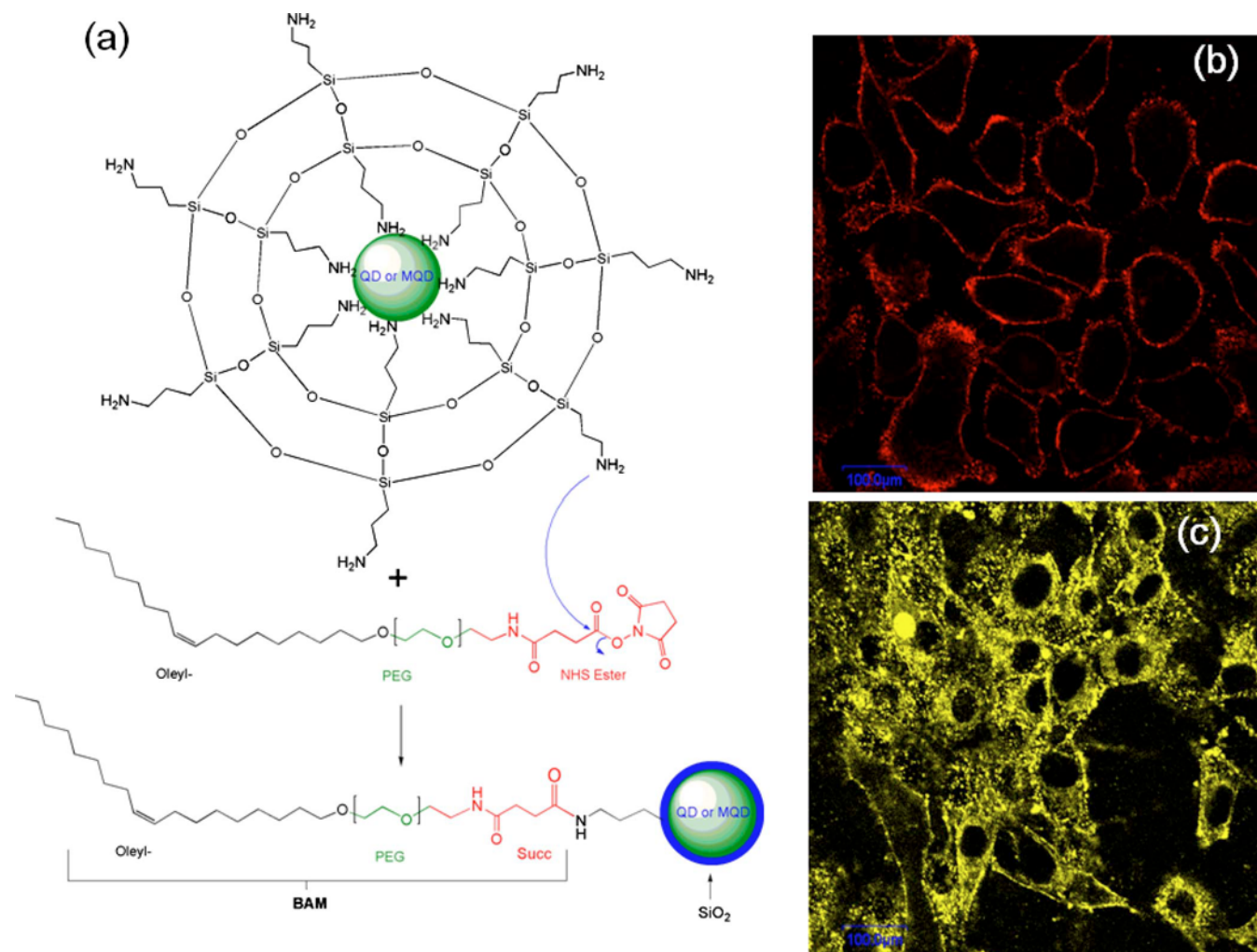


FIG. 2. (Color online) (a) Scheme depicting the silica-coated CdSe QDs in reverse microemulsion and dispersed NPs in phosphate buffered saline buffer. The surface  $\text{NH}_2$  groups are then reacted with BAM to form a covalent amide bond. The oleyl groups are used to anchor to the cell membrane in biolabeling. [(b) and (c)] CLSM images showing the labeling of (b) HepG2 and (c) NIH-3T3 cell membranes, using BAM/SiO<sub>2</sub>/CdSe QDs. Adapted from Ref. 6 with permission. Copyright 2007, Wiley-VCH.

groups of APS were hydrolyzed and condensed with another APS, exposing surface amine groups on the silanized QDs (SiO<sub>2</sub>/QDs) for conjugation with oleyl-O-poly(ethyleneglycol)-succinyl-N-hydroxysuccinimidyl ester, denoted as bioanchored membrane (BAM) [Fig. 2(a)]. The reaction between the amine group and NHS ester resulted in a covalent amide bond formation, leaving the exposed oleyl group for the effective targeting of cell membrane. Figures 2(b) and 2(c) show the confocal laser scanning microscopy (CLSM) images of different cell membranes labeled with BAM/SiO<sub>2</sub>/CdSe QDs. The labeling of live cell membranes (HepG2 human liver cancer cells and NIH-3T3 mouse fibroblast cells) indicated the successful conjugation of silica-coated QDs with BAM.<sup>6</sup>

### III. ADVANCES IN MULTIFUNCTIONAL NANOPARTICLES

Multifunctional NPs have been actively explored for the enhancement of imaging, targeting, and delivery. In the field

of biological and biomedical imaging, QDs and MPs have been enjoying greater roles in biolabeling<sup>1</sup> and MRI,<sup>31</sup> respectively. A combination of optical and magnetic properties in a single material would enable the simultaneous biolabeling/imaging and cell sorting/separation.<sup>18,32</sup>

MPs less than 15 nm in size display superparamagnetic characteristics, which are important for applications such as MRI, magnetically guided site-specific drug delivery, and ac magnetic field assisted cancer therapy.<sup>33</sup> In recent years, researchers have focused on the synthesis of highly uniform size iron oxide NPs, particularly magnetite (Fe<sub>3</sub>O<sub>4</sub>) and maghemite ( $\gamma$ -Fe<sub>2</sub>O<sub>3</sub>). We have reported a gram-scale synthesis of nearly monodispersed  $\gamma$ -Fe<sub>2</sub>O<sub>3</sub> (maghemite) nanoclusters with a less expensive oxidant and without a hazardous iron pentacarbonyl [Fe(CO)<sub>5</sub>] or iron acetylacetonate precursor.<sup>34</sup>

Biomagnetic NPs consisting of ferritin protein were conjugated to carboxyl-coated QDs (QD525, QD655, and QD800 from Invitrogen) using 1-ethyl-3-(3-

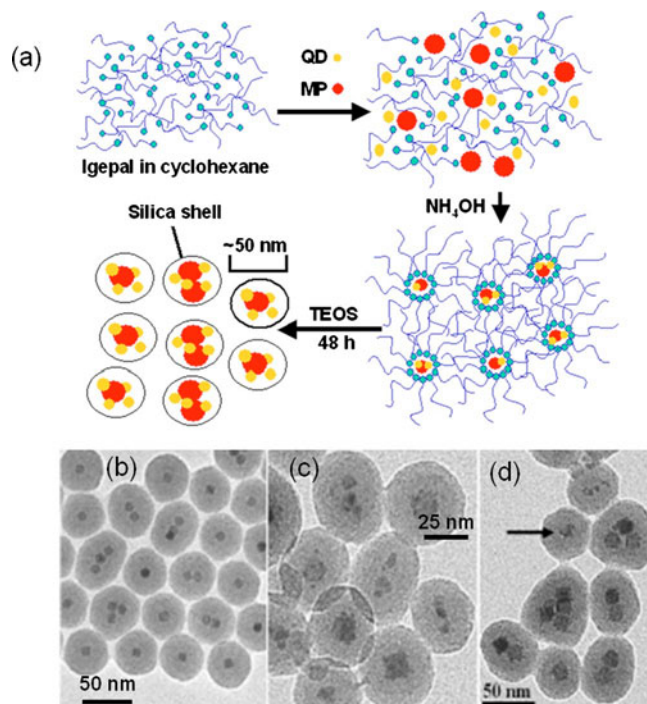


FIG. 3. (Color online) (a) Scheme depicting the encapsulation of QDs and MPs within silica shells. TEM images of (b)  $\gamma$ -Fe<sub>2</sub>O<sub>3</sub> MPs and [(c) and (d)] hybrid core NPs consisting of CdSe QDs and  $\gamma$ -Fe<sub>2</sub>O<sub>3</sub> MPs encapsulated within silica shells. Adapted from Ref. 29 with permission. Copyright 2005, ACS.

dimethylaminopropyl) carbodiimide hydrochloride coupling.<sup>35</sup> To improve the biocompatibility of silica NPs, poly(ethyleneglycol) (PEG)-phospholipids were coated onto silica NPs containing QDs and paramagnetic Gd-DTPA and used for multimodality imaging.<sup>36</sup> The PEG-lipid coated silica NPs administered into mice increased the blood circulation half-life time of NPs by a factor of 10. These multifunctional silica NPs could be used for drug delivery, gene therapy, and molecular imaging. Recently, uniform mesoporous dye-doped silica decorated with multiple magnetite NPs have been developed for simultaneous enhanced magnetic resonance imaging, fluorescence imaging, and drug delivery applications.<sup>37</sup>

We have developed several approaches for the fabrication of multifunctional NPs. In the following sections, we describe the synthesis and application of (a) silica-coated nanocomposites of fluorescent QDs and MPs, (b) seed-mediated synthesis of fluorescent QDs and MPs, and (c) rare earth probes as multimodal contrast agents.

### A. Silica-coated nanocomposites of fluorescent QDs and MPs

In 2005, we reported an elegant method to incorporate QDs and MPs within silica using a reverse microemulsion method.<sup>29</sup> The scheme in Fig. 3(a) depicts the synthesis of silica-coated nanocomposites of MPs and QDs. Single or multiple MPs (Fig. 3(b)) can be encapsulated within each silica shell. The silica shell thickness can be altered by vary-

ing the TEOS concentration. Varying the amount of water and ammonia in the microemulsion also affected the silica shell thickness, since this altered the aqueous domain size. The encapsulated MPs are monodispersed ( $11.8 \pm 1.3$  nm in diameter) and multiple (single, double, and triple) MPs are clearly seen in the image [Fig. 3(b)].<sup>29</sup> In our microemulsion synthesis, MPs ( $\sim 11.8$  nm) and QDs ( $\sim 3.5$  nm) were encapsulated within spherical silica shells after 48 h of reaction, yielding SiO<sub>2</sub>/MP-QD NPs. The quantum yield of these composite NPs increased from 3.2% (in the absence of ZnS) to 4.8% in the presence of ZnS capping. The low quantum yield might be attributed to the quenching by MPs. After the encapsulation of QDs and MPs, silica NPs appeared to be elongated [Figs. 3(c) and 3(d)]. Energy dispersive x-ray analysis confirmed the presence of CdSe, Fe<sub>2</sub>O<sub>3</sub>, and silica.

### B. Seed-mediated synthesis of fluorescent QDs and MPs

Bifunctional NPs consisting of QDs and MPs, known as magnetic quantum dots (MQDs), are emerging as a versatile system for both fluorescence and magnetic based applications. Recently, we have developed a seed-mediated synthesis of MQDs by growing CdSe QDs on Fe<sub>2</sub>O<sub>3</sub> cores, yielding either heterodimers or a homogeneous dispersion of QDs around Fe<sub>2</sub>O<sub>3</sub>. This method allows for flexibility in tuning the optical and magnetic properties separately.<sup>6</sup> At first, Fe<sub>2</sub>O<sub>3</sub> MPs were synthesized in oleic acid and dioctyl ether by the decomposition of iron pentacarbonyl. In the growth solution, CdSe QDs were allowed to grow for different time periods (1–5 min) to yield different dot sizes that corresponded to green, yellow, orange, and red emissions. The synthesis and purification procedures were detailed in Ref. 6.

In another interesting work, we have demonstrated a versatile one-pot approach for the synthesis of Fe<sub>2</sub>O<sub>3</sub>-CdSe MQDs with a high quantum yield of up to 42%. The as-synthesized nanocomposite particles remained stable in non-polar solvents, such as chloroform and hexane. Addition of methanol destabilized the suspension, and both QDs and MPs were attracted to a magnet placed close to the suspension [Figs. 4(a) and 4(b)]. When methanol was added, both the MPs and QDs were believed to be aggregated and separated by the magnet, due to either the presence of dimers or the formation of the hydrophobic bilayer, utilizing the interaction of the surfactants (octadecyl amine on the MP surface and TOPO on the QD surface). The aggregated particles, which were both fluorescent and magnetic, could be redispersed in chloroform [Fig. 4(c) inset]. The emission peaks became broader with an increase in growth time from 1–12 to 25–30 min [Fig. 4(c)], indicating that the particle aggregation was induced by either bilayer or heterodimer formation. It is important to note that different QD growth rates during the reaction period might also be responsible for emission-peak broadening.

### C. RE NPs as multimodal contrast agents

For a wide range of biological applications, silica coating is an effective means to protect or modify the surface of RE

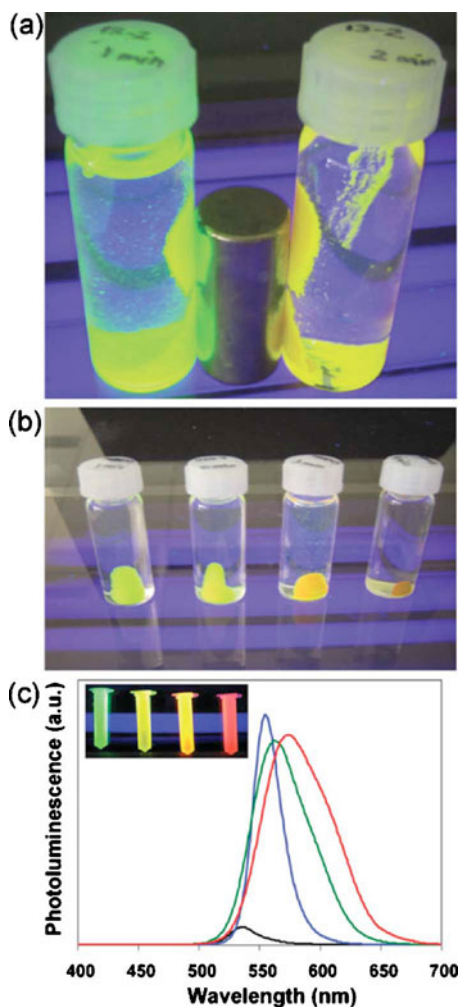


FIG. 4. (Color online) [(a) and (b)] Photographs of magnetically harvested particles under UV excitation at 365 nm. (c) Photoluminescence spectra of  $\text{Fe}_2\text{O}_3$ -CdSe MQDs obtained after different growth periods of 1–30 min and (inset) chloroform-dispersed MQDs. Adapted from Ref. 34 with permission. Copyright 2009, Wiley-VCH.

NPs. Reverse microemulsion has been conveniently employed to coat hydrophobic  $\text{Y}_2\text{O}_3$ ,<sup>38</sup>  $\text{YF}_3$ ,<sup>39</sup> and  $\text{NaYF}_4$  (Ref. 40) NPs with silica. Multicolor spheres were produced by encapsulating organic dyes or QDs into the silica shell, and up-conversion fluorescence was generated based on fluorescence resonance energy transfer from the  $\text{NaYF}_4$  cores to organic dyes or QDs. The silica-coated NPs were dispersible in water and showed good colloidal and photochemical stability.

Silica coating of RE NPs also provides a facile route to construct multicolor NPs when organic dyes or other fluorescent QDs are encapsulated within the silica shell. Due to their sharp emission peaks and long life time, RE NPs act as good energy donors to organic dyes or QDs. A similar reverse microemulsion system was used to construct multicolor dye/QD doped  $\text{NaYF}_4$ :Yb,Er/Tm at  $\text{SiO}_2$  NPs.<sup>40</sup> In such NPs, NIR radiation absorbed by the up-conversion NPs (the core) at a single wavelength (980 nm) is converted to visible fluorescence, which in turn is absorbed by the down-

conversion materials (embedded in the shell) to emit multi-color fluorescence. The characteristic visible colors from the dyes and QD605, which are generally excited under blue light, could clearly be seen when these NPs are excited with a 980 nm NIR laser.

Very recently, UCNPs are emerging as a new type of multimodal imaging probe for both optical imaging and MRI.<sup>40,41</sup> The deep penetration depth of NIR excitation, excellent photostability, nonblinking, and absence of autofluorescence of UCNPs make them attractive imaging probes for applications such as targeting of tumor tissues *in vivo* and long-term cellular and animal imaging.

Very recently, we have reported a simple strategy for synthesizing paramagnetic-fluorescent ultranarrow gadolinium oxide nanorods (NRs) as multimodal contrast agents.<sup>42</sup> The room temperature photoluminescence spectra of the Tb-doped  $\text{Gd}_2\text{O}_3$  NRs excited at 235 nm showed down-conversion emission. The characteristic emission peaks of Tb ions appeared at 489, 545, 585, and 619 nm. To demonstrate the versatility of the RE ion doping approach for up-conversion emission, we doped the NRs with Yb and Er ions. The up-conversion luminescence of Yb-/Er-codoped  $\text{Gd}_2\text{O}_3$  NRs showed green emissions at 520 and 539 nm at 980 nm excitation. The room temperature magnetization of  $\text{Gd}_2\text{O}_3$ :RE (RE=Tb, Yb/Er), as a function of applied field (from  $-10$  to  $+10$  kOe), showed a linear correlation with a magnetization value of 2.46 emu/g (at 10 kOe), suggesting that the  $\text{Gd}_2\text{O}_3$ :RE NRs are paramagnetic.

Down-conversion and up-conversion fluorescence can be achieved by changing the lanthanide dopants, as shown in Figs. 5(a) and 5(b). Furthermore, the Yb-/Er-codoped  $\text{Gd}_2\text{O}_3$  NPs exhibited good  $T_1$ -weighted MRI contrast, comparable to the commercial product Gadovist [Fig. 5(c)].

#### IV. CONCLUDING REMARKS

Over the decade, the application of QDs in biolabeling has been emerging as a matured technology especially in cell based imaging. Cadmium is basically carcinogenic, and therefore, the *in vivo* applications still concern the toxicity of QDs. Robust coating methods have shown the nontoxicity of QDs in *in vitro* studies. However, the size, charge, and coating material of QDs dictate the cell uptake and clearance as demonstrated in recent studies.<sup>43,44</sup> Multifunctional NPs possessing fluorescent, magnetic, and targeting functionalities are useful in biomedical research. Although there are considerable advances in recent years, the application of multifunctional NPs in *in vivo* imaging is still in its infancy. This invites the development of more multifunctional systems with less toxic fluorescent probes, excluding carcinogenic elements such as Cd and Pb. The size of the NPs plays a critical role in cellular uptake and tumor-targeting. If the size is small ( $<10$  nm), the NPs could be excreted from the animal body easily. In order to minimize the overall size of QDs or multifunctional NPs, a thin hydrophilic shell should be grown. The reverse microemulsion method can be employed to achieve a thin silica or polymer shell, which can be further functionalized with biomolecules of interest. The RE-doped

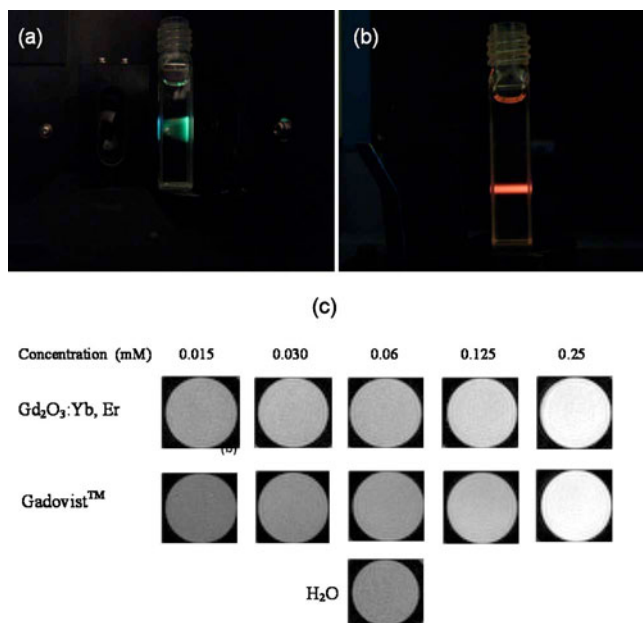


FIG. 5. (Color online) Digital photographs of (a) down-conversion Tb-doped  $Gd_2O_3$  solution exhibiting green emission at 235 nm excitation and (b) up-conversion Yb/Er-codoped  $Gd_2O_3$  solution exhibiting red emission at 980 nm excitation. (c)  $T_1$ -weighted images of  $Gd_2O_3$ :Yb,Er and Gadovist at various  $Gd^{3+}$  concentrations.  $T_1$ -weighted image of water sample is shown as reference. Adapted from Ref. 42 with permission. Copyright 2010, ACS.

UCNPs are emerging as an alternative candidate system for bioimaging applications.

The challenge that we face in the future would involve the development of “smart” contrast agents that are capable of monitoring specific cellular and molecular events *in vivo*. Our current work is focused on the development of versatile multifunctional paramagnetic NPs for multimodality imaging in a number of clinical pathologies such as early cancer diagnosis and cellular trafficking in stem cell therapy and immunological interventions. The targeted delivery of drugs is an important area in health care. By conjugating multiple components such as fluorescent QDs or dyes or UCNPs, tumor-targeting groups, anticancer drugs, or siRNA to the MPs, future work would seek to provide solutions to early cancer diagnosis and targeted delivery of therapeutics.

## ACKNOWLEDGMENTS

The author would like to thank all the students and researchers who have contributed to the work described in this article. This work is supported by A\*STAR (Agency for Science, Technology and Research), Singapore, Joint Council Office (JCO) Grant No. JCOAG03\_FG03\_2009.

<sup>1</sup>I. L. Medintz, H. T. Uyeda, E. R. Goldman, and H. Mattoussi, *Nature Mater.* **4**, 435 (2005).

<sup>2</sup>X. Michalet *et al.*, *Science* **307**, 538 (2005).

<sup>3</sup>X. Gao, L. Yang, J. A. Petros, F. F. Marshall, J. W. Simons, and S. Nie, *Curr. Opin. Biotechnol.* **16**, 63 (2005).

- <sup>4</sup>A. P. Alivisatos, W. Gu, and C. Larabell, *Annu. Rev. Biomed. Eng.* **7**, 55 (2005).
- <sup>5</sup>S. T. Selvan, T. T. Tan, and J. Y. Ying, *Adv. Mater.* **17**, 1620 (2005).
- <sup>6</sup>S. T. Selvan, P. K. Patra, C. Y. Ang, and J. Y. Ying, *Angew. Chem., Int. Ed.* **46**, 2448 (2007).
- <sup>7</sup>H. L. Zhang, Y. Q. Li, J. H. Wang, X. N. Li, S. Lin, Y. D. Zhao, and Q. M. Luo, *J. Biomed. Opt.* **15**, 015001 (2010).
- <sup>8</sup>R. Kumar, H. Ding, R. Hu, K. T. Yong, I. Roy, E. J. Bergey, and P. N. Prasad, *Chem. Mater.* **22**, 2261 (2010).
- <sup>9</sup>S. J. Tan, N. R. Jana, S. J. Gao, P. K. Patra, and J. Y. Ying, *Chem. Mater.* **22**, 2239 (2010).
- <sup>10</sup>R. Weissleder, *Science* **312**, 1168 (2006).
- <sup>11</sup>S. R. Dave and X. H. Gao, *Wiley Interdiscip. Rev.-Nanomedicine Nanobiotechnol.* **1**, 583 (2009).
- <sup>12</sup>H. Tan, J. M. Xue, B. Shuter, X. Li, and J. Wang, *Adv. Funct. Mater.* **20**, 722 (2010).
- <sup>13</sup>C. Vogt, M. S. Toprak, M. Muhammed, S. Laurent, J. L. Bridot, and R. N. Muller, *J. Nanopart. Res.* **12**, 1137 (2010).
- <sup>14</sup>S. T. Selvan, T. T. Y. Tan, D. K. Yi, and N. R. Jana, *Langmuir* **26**, 11631 (2010).
- <sup>15</sup>A. Guerrero-Martínez, J. Pérez-Juste, and L. M. Liz-Marzán, *Adv. Mater.* **22**, 1182 (2010).
- <sup>16</sup>J. F. Wang, T. Tsuzuki, L. Sun, and X. G. Wang, *ACS Appl. Mater. Inter.* **2**, 957 (2010).
- <sup>17</sup>L. Zhou, C. Gao, X. Z. Hu, and W. J. Xu, *ACS Appl. Mater. Inter.* **2**, 1211 (2010).
- <sup>18</sup>V. Salgueiriño-Maceira, M. A. Correa-Duarte, M. Spasova, L. M. Liz-Marzán, and M. Farle, *Adv. Funct. Mater.* **16**, 509 (2006).
- <sup>19</sup>T. T. Tan, S. T. Selvan, Z. Lan, S. Gao, and J. Y. Ying, *Chem. Mater.* **19**, 3112 (2007).
- <sup>20</sup>T. Pellegrino *et al.*, *Nano Lett.* **4**, 703 (2004).
- <sup>21</sup>N. R. Jana, C. Earhart, and J. Y. Ying, *Chem. Mater.* **19**, 5074 (2007).
- <sup>22</sup>D. Gerion, F. Pinaud, S. C. Williams, W. J. Parak, D. Zanchet, S. Weiss, and A. P. Alivisatos, *J. Phys. Chem. B* **105**, 8861 (2001).
- <sup>23</sup>J. Aldana, N. Lavelle, Y. Wang, and X. Peng, *J. Am. Chem. Soc.* **127**, 2496 (2005).
- <sup>24</sup>H. Duan and S. Nie, *J. Am. Chem. Soc.* **129**, 3333 (2007).
- <sup>25</sup>X. Wu, H. Liu, J. Liu, K. N. Haley, J. A. Treadway, J. P. Larson, N. Ge, F. Peale, and M. P. Bruchez, *Nat. Biotechnol.* **21**, 41 (2003).
- <sup>26</sup>B. Dubretret, P. Skourides, D. J. Norris, V. Noireaux, A. H. Brivanlou, and A. Libchaber, *Science* **298**, 1759 (2002).
- <sup>27</sup>K. Susumu, H. T. Uyeda, I. L. Medintz, T. Pons, J. B. Delehanty, and H. Mattoussi, *J. Am. Chem. Soc.* **129**, 13987 (2007).
- <sup>28</sup>P. Mulvaney, L. M. Liz-Marzán, M. Giersig, and T. Ung, *J. Mater. Chem.* **10**, 1259 (2000).
- <sup>29</sup>D. K. Yi, S. T. Selvan, S. S. Lee, G. C. Papaefthymiou, D. Kundaliya, and J. Y. Ying, *J. Am. Chem. Soc.* **127**, 4990 (2005).
- <sup>30</sup>R. Koole, M. M. van Schooneveld, J. Hilhorst, C. D. Donega D. C. 't Hart, A. van Blaaderen, D. Vanmaekelbergh, and A. Meijerink, *Chem. Mater.* **20**, 2503 (2008).
- <sup>31</sup>I. J. de Vries *et al.*, *Nat. Biotechnol.* **23**, 1407 (2005).
- <sup>32</sup>A. Quarta, R. D. Corato, L. Manna, A. Ragusa, and T. Pellegrino, *IEEE Trans. Nanobiosci.* **6**, 298 (2007).
- <sup>33</sup>Y. Lee, J. Lee, C. J. Bae, J. G. Park, H. J. Noh, J. H. Park, and T. Hyeon, *Adv. Funct. Mater.* **15**, 503 (2005).
- <sup>34</sup>C. Y. Ang, L. Giam, Z. M. Chan, A. W. H. Lin, H. Gu, E. Devlin, G. C. Papaefthymiou, S. T. Selvan, and J. Y. Ying, *Adv. Mater.* **21**, 869 (2009).
- <sup>35</sup>B. Fernández, N. Gálvez, R. Cuesta, A. B. Hungria, J. J. Calvino, and J. M. Domínguez-Vera, *Adv. Funct. Mater.* **18**, 3931 (2008).
- <sup>36</sup>M. M. van Schooneveld *et al.*, *Nano Lett.* **8**, 2517 (2008).
- <sup>37</sup>J. E. Lee *et al.*, *J. Am. Chem. Soc.* **132**, 552 (2010).
- <sup>38</sup>G. K. Das and T. T. Y. Tan, *J. Phys. Chem. C* **112**, 11211 (2008).
- <sup>39</sup>M. Darbandi and T. Nann, *Chem. Commun. (Cambridge)* **7**, 776 (2006).
- <sup>40</sup>Z. Q. Li, Y. Zhang, and S. Jiang, *Adv. Mater.* **20**, 4765 (2008).
- <sup>41</sup>Y. Zhang, G. K. Das, R. Xu, and T. T. Y. Tan, *J. Mater. Chem.* **19**, 3696 (2009).
- <sup>42</sup>G. K. Das *et al.*, *Langmuir* **26**, 8959 (2010).
- <sup>43</sup>Y. Wei, N. R. Jana, S. J. Tan, and J. Y. Ying, *Bioconjugate Chem.* **20**, 1752 (2009).
- <sup>44</sup>H. S. Choi, W. Liu, P. Misra, E. Tanaka, J. P. Zimmer, B. I. Ipe, M. G. Bawendi, and J. V. Frangioni, *Nat. Biotechnol.* **25**, 1165 (2007).